REGOLITH CHARACTERISATION USING ASTER DATA IN THE CENTRAL NAMIB, NAMIBIA

Kombada Mhopjeni[1, 2], Thomas Cudahy[3], Arianne Ford[1], Carsten Laukamp[3] and Campbell McCuaig[1]

1. School of Earth and Environment and Centre for Exploration and Targeting, University of Western Australia, Perth, Australia
2. Geological Survey of Namibia, Ministry of Mines and Energy, Windhoek, Namibia
3. WA Centre of Excellence for 3D Mineral Mapping, CSIRO Earth Science and Resource Engineering, Perth, Australia

1. INTRODUCTION

Multi-spectral remote Advanced Spaceborne Thermal Emission and Reflection Radiometer (ASTER) sensor is an inexpensive, powerful remote sensing tool for measuring mineral group abundance and composition of surface materials [1]. The published geological map of the central Namib Uranium District (CNUD) contains tracts of Quaternary cover sediments that are largely mapped as an undifferentiated unit [2]. Hyper-arid to semi-arid environments with minimum vegetation cover are ideal for the use of spectral remote sensing technologies. The study area is located within the central part of the Namib Desert along the central west coast of Namibia (Figure 1a). The published geology of central Namib comprises Palaeoproterozoic gneissic basement and Neoproterozoic Damara Supergroup metasediments, and associated intrusive rocks, overlain by Quaternary to recent surficial deposits [2, 3]. The main aim of this study was to mineralogically discriminate and map the undifferentiated Quaternary regolith using ASTER data (Figure 1b). Mapping the surficial cover sediments has potential benefits such as contributing to the understanding of the provenance of the surficial sediments and providing enhanced base-line data that can further aid mineral exploration in the region.

2. DATA AND METHODS

Level 1B and L3A ASTER data were used for mapping the regolith mineralogy. Airborne hyperspectral HyMap data were down-sampled to ASTER spectral and spatial resolution, for comparison with ASTER data. A co-registered visible and near infrared (VNIR) and shortwave infrared (SWIR) ASTER image was cross-calibrated through linear regression method using reflectance HyMap imagery [1, 4]. The calibrated reflectance ASTER VNIR-SWIR scene was used to

transform the remaining radiance ASTER scenes. No pre-processing was applied to the thermal infrared (TIR) bands. Mosaicking and masking were applied to the ASTER data.

Several ASTER mineral maps were produced from the calibrated ASTER reflectance and uncalibrated thermal radiance data using spectral band ratios and relative band depth (RBD) (Table 1.). Resampled hyperspectral (HyMap, ASD and PIMA), and XRD data, and field observations were used to compare and validate the ASTER products.

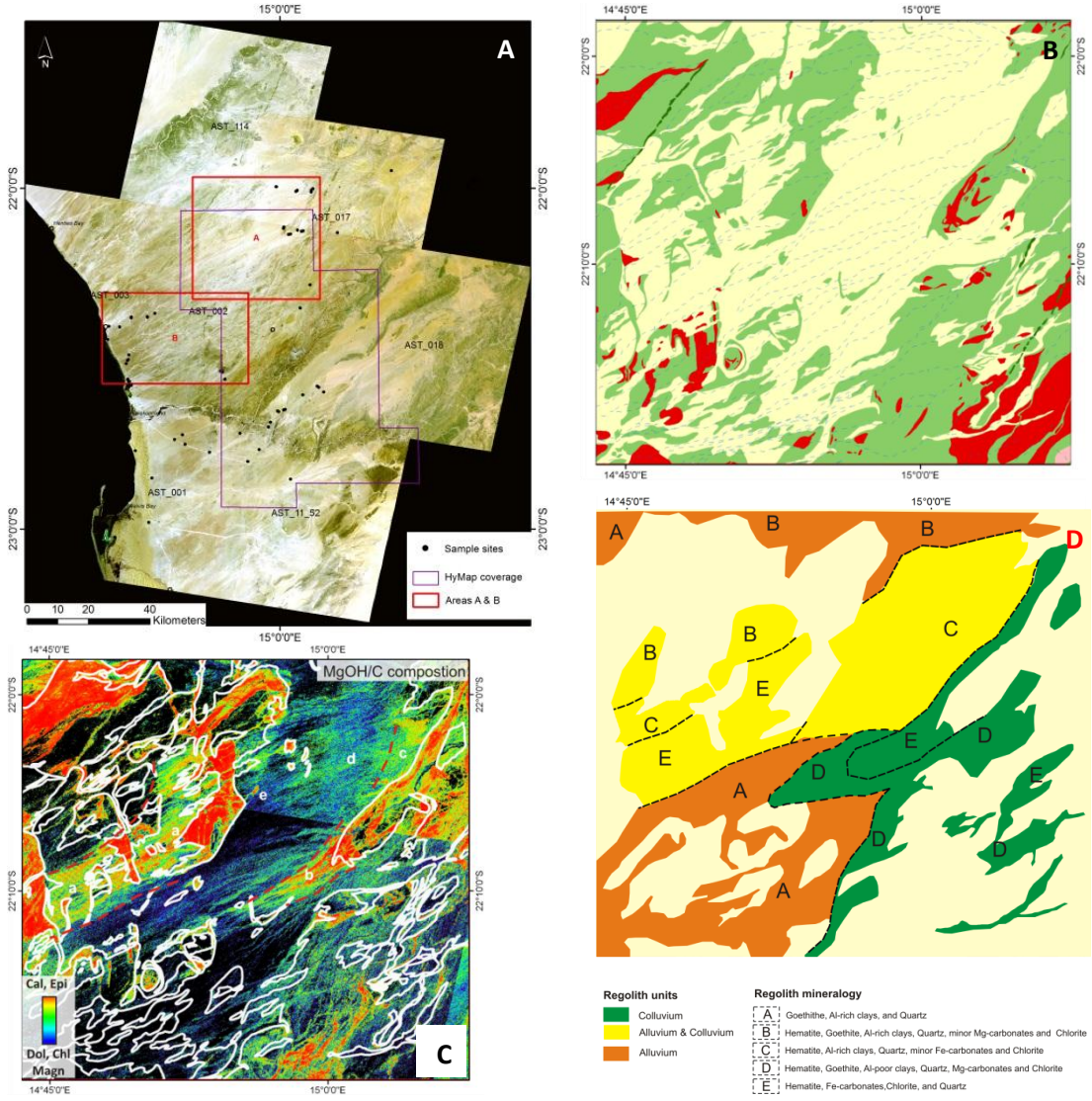

Figure 1. A) Calibrated ASTER VNIR-SWIR false colour RGB (321) mosaic indicating the HyMap coverage (purple), sample sites and the study sites (Inland, A and Coastal, B) used to map regolith mineralogy in detail. B) Published geological map with uniform Quaternary unit ('yellow'), Neoproterozoic Damara sediments (in green) and intrusives (in red). C) MgOH/C composition ASTER mineral map for the Inland sub-site (A). Cal = calcite, Epi = epidote, Dol = dolerite, Chl = chlorite, and Magn = magnesite. D) Interpreted, new regolith units for the inland area.

Table 1. Mineral spectral indices used in the study.

ASTER Product	Band ratio/ RDB	Minerals Covered
AlOH composition	B5/B7	Blue = Al-rich clays, Red = Al-poor clays
AlOH content	(B5+B7)/B6	AlOH clays e.g. phengite, muscovite, illite, kaolin
Ferric oxide content	B4/B3	Hematite, goethite, jarosite
Ferric oxide composition	B2/B1	Blue = Goethite-rich, Red = Hematite-rich
Ferrous iron Index	B5/B4	Ferrous iron in carbonates and/or silicates e.g. ankerite
Kaolin Index	B6/B5	Kaolinite, dickite, pyrophyllite, alunite
MgOH/C composition	B7/B8	Blue = e.g. dolomite, chlorite Red = calcite, epidote
MgOH/C content	(B6+B9)/(B7+B8)	MgOH/C minerals e.g. calcite, dolomite, chlorite, amphibole
Ferrous iron in MgOH/C	B5/B4	Fe-chlorite, actinolite, siderite, ankerite
FeOH content	(B6+B8)/B7	FeOH minerals e.g. chlorite, nontronite, gypsum
Carbonate Index	B13/B14	Carbonate e.g. calcite, dolomite and siderite
Mafic Index	B12/B13	Pyroxenes, garnets, epidote, chlorite
Quartz Index	B11/(B10+B12)	Quartz

Sources: [1, 4, 5, 6]

* B = Band, MgOH/C = carbonate and/or MgOH.

3. RESULTS

3.1. ASTER Mineral Maps

Band ratios and relative band depth ratio (RBD, Table 1) were applied to calibrated ASTER VNIR-SWIR reflectance imagery and uncalibrated ASTER TIR radiance imagery, to produce mineral maps targeting common regolith minerals (e.g. clays, iron oxides and quartz). For example the ASTER AlOH ratio ((B5+B7)/B6) provides information on the Al-OH clay mineral abundance. Similarly, the MgOH/C products (B7/B8, (B6+B9)/ (B7+B8)) are sensitive to carbonates and Mg-OH bearing minerals (Figure 1c). Overall, the ASTER mineral maps show favourable agreement with the additional datasets, with the majority of the important relevant minerals detected. Several spectral mineralogical trends are present in the ASTER derived mineral maps compared to the current geological map, in the Quaternary cover.

3.2. Regolith Mapping

Two main sub-areas, inland and coastal were focussed on. Four regolith units (colluvium, alluvium, alluvium-aeolian, and alluvium-colluvium) and seven mineralogical zones were identified through integrated spectral analysis of ASTER geoscience products. Figure 1d shows the inland site which is dominated by alluvial cover sediments and here the regolith is transported SW, mainly by fluvial systems. In contrast, the coastal area (B) has four regolith units (including the alluvium-aeolian). The coastal area has major alluvial and aeolian cover sediments. The coastal regolith materials are transported NE and SW, by aeolian and fluvial processes, respectively.

4. CONCLUSIONS

The study was successful in further characterising the Quaternary surficial sediments based on spectral mineralogy, currently denoted as the undifferentiated cover in the published geology. Based on the analysis and interpretation of the spectral mineralogy, the provenance of the cover sediments was established. Multiple sources, including local bedrock and distal marine sources contributed to the development of the Quaternary sediments in the region. The study also provides a framework and opportunity for future work, such as and mapping of a larger area. Further evaluation of the spatial accuracy of interpreted units in the field is needed.

5. REFERENCES

[1] Hewson, R.D., Cudahy, T.J., Mizuhiko, S., Ueda, K., & Mauger, A.J. (2005). Seamless geological map generation using ASTER in the Broken Hill-Curnamona province of Australia. Remote Sensing of Environment, 99, 159-172.

[2] Geological Survey of Namibia (1995). 1:250 000 Geological Map Series - Walvis Bay sheet (2214).

[3] Miller, R.M. (2008). The Geology of Namibia. Windhoek: Ministry of Mines and Energy, Geological Survey of Namibia.

[4] Cudahy, J.T., Jones, M., Thomas, M., Laukamp, C., Caccetta, M., Hewson, D.R., Rodger, A., & Verrall, M. (2008). Next Generation Mineral Mapping: Queensland Airborne HyMap and Satellite ASTER Surveys 2006-2008. In, CSIRO Exploration & Mining Report P2007 / 364. Perth: CSIRO.

[5] Rowan, L.C., & Mars, J.C. (2003). Lithologic mapping in the Mountain Pass, California area using Advanced Spaceborne Thermal Emission and Reflection Radiometer (ASTER) data. Remote Sensing of Environment, 84, 350-366.

[6] Ninomiya, Y., Fu, B., & Cudahy, T.J. (2005). Detecting lithology with Advanced Spaceborne Thermal Emission and Reflection Radiometer (ASTER) multispectral thermal infrared "radiance-at-sensor" data. Remote Sensing of Environment, 99, 127-139.